Title

Contrasting the hydrologic response due to land cover and climate change in a mountain headwaters system

Journal

Ecohydrology, 9(8)

ISSN

1936-0584

Authors

Pribulick, Christine E
Foster, Lauren M
Bearup, Lindsay A
et al.

Publication Date

2016-12-01

DOI

10.1002/eco.1779

Peer reviewed

Contrasting the hydrologic response due to land cover and climate change in a mountain headwaters system

Christine E. Pribulick, Lauren M. Foster, Lindsay A. Bearup, Alexis K. Navarre-Sitchler, Kenneth H. Williams, Rosemary W.H. Carroll, Reed M. Maxwell

First published: 25 August 2016
https://doi.org/10.1002/eco.1779

Abstract

Land cover change due to drought and insect-induced tree mortality or altered vegetation succession is one of the many consequences of anthropogenic climate change. While the hydrologic response to land cover change and increases in temperature have been explored independently, few studies have compared these two impacts in a systematic manner. These changes are particularly important in snow-dominated, headwaters systems that provide streamflow for continental river systems. Here we study the hydrologic impacts of both vegetation change and climate warming along three transects in a mountain headwaters watershed using an integrated hydrologic model. Results show that while impacts due to warming generally outweigh those resulting from vegetation change, the inherent variability within the transects provides varying degrees of response. The combination of both vegetation change and warming results in greater changes to streamflow amount and timing than either impact individually, indicating a nonlinear response from these systems to multiple perturbations. The complexity of response underscores the need to integrate observational data and the challenge of deciphering hydrologic impacts from proxy studies.

1 INTRODUCTION

The Earth is experiencing substantial vegetation change (Hansen et al., 2013) driven by changes in climate, insect infestation, and land use (Bradford, Birdsey, Joyce, & Ryan, 2008, Allen et al., 2010, Edburg et al., 2012, Williams et al., 2013). Understanding how a catchment will respond to vegetation change is important as it can alter hydrologic systems by modifying flow path contribution to streams, altering snowpack accumulation and depletion, and impacting water vapor exchange with the atmosphere (Bradford et al., 2008, Bearup, Maxwell, Clow, & McCray, 2014, Penn, Bearup, Maxwell, & Clow, 2016). The Colorado River is a major water source and economic engine for much of the western United States with 90% of its water originating from the snow-dominated upper watersheds in Colorado, Utah, and Wyoming (Bales et al., 2006). Confounding the hydrologic effects of vegetation perturbations in these systems, climate change is expected to decrease flows between 5 and 20% in the next 40 years (Vano et al., 2013) due to decreased nowpack in the Rocky Mountains (Bradford et al., 2008, Clow, 2009, Lukas, Barsugli, Rangwala, & Woler, 2014), longer lasting droughts, and increased temperatures.

Field studies and model projections are the two main ways to predict future response of mountain ecosystems to climate change. Observational studies have assessed climate impacts in snowmelt-dominated systems using proxies such as elevation or latitude (Berghuijs, Woods, & Hrachowitz, 2014, Goulden & Bales, 2014) and field manipulations to assess vegetative shifts in relation to climate change (Harte & Shaw, 1995). Similar modeling

work to this study has been conducted on specific components of hydrologic response to climate change. A recent study on the sensitivity of mountain hydrology to climate-driven changes in the phase of precipitation highlights the importance of energy increases on hydrologic partitioning in snow-dominated watersheds (Foster, Bearup, Molotch, Brooks, & Maxwell, 2016). Furthermore, different warming and drying scenarios result in different recharge patterns for different geologic settings of mountain regions, with greater susceptibility to climate change occurring in areas with greater subsurface water retention (Markovich, Maxwell, & Fogg, 2016).

Building on this prior work, this study uses an integrated hydrologic model to study hydrologic changes as a result of both large-scale climatic change and vegetative shifts. Despite the availability of analogs such as logging, fire, and infestation, recent work has suggested different governing processes across scales may result in different hydrologic conditions after disturbance (Adams et al., 2012, Biederman et al., 2014, Penn et al., 2016). Few studies have attempted to isolate the effects of climate-specific vegetation change from the increases in temperature that drive these changes. Here, a series of numerical experiments are conducted with a perturbed future climate scenario along with vegetative shifts corresponding to observations from induced-warming plot experiments (Harte & Shaw, 1995). These numerical experiments were conducted along three representative transects to study a range of connected hydrologic response.

2 METHODS

The integrated, hydrologic model ParFlow was used for this study. ParFlow solves for surface and subsurface flow using the three-dimensional Richards' equation and the shallow water equations simultaneously (Kollet & Maxwell, 2006). ParFlow is also coupled to a land surface model (derived from CLM 3.5, this model is often referred to as ParFlow-CLM), which simulates the land surface water and energy budgets. Incoming precipitation is initially partitioned between the canopy and ground surface based on the maximum canopy storage of 0.1 mm of liquid water equivalent distributed over the leaf area index (LAI) (Penn et al., 2016). Water and energy fluxes from soil, snow, and leaf surfaces (i.e., evaporation/sublimation and sensible heat exchange) are simulated using a mass transfer approach that applies the Monin-Obukhov theorem to account for atmospheric instability. Soil evaporation is also limited using a beta formulation based on soil moisture (Jefferson & Maxwell, 2015). Transpiration occurs from the canopy fraction that is dry and not buried by snow and accounts for stomatal and aerodynamic resistances. Transpiration may be limited by light, enzyme, or moisture availability; the latter represented by a parameterized function of the rooting fraction in each soil layer (Table 1; (Jefferson, Gilbert, Constantine, & Maxwell, 2015)). This coupled system is driven by hourly observed meteorology forcing as described below.

Table 1. Select vegetation properties capturing the vegetation shift from grass to shrubs, including leaf area index (LAI), which changes seasonally within the range provided, stem area index (SAI), root distribution parameters (a, b), and aerodynamic roughness length (z0)

Vegetation type	LAI [−]	SAI [−]	$f_{root} = 1-0.5[e^{-az} + e^{-bz}]$		z0 [m]
			a	b	
Grass	0.5–2	4	1	2.5	0.03
Shrubs	1–6	2	5	2.5	0.1

The focus of this study is the East River headwaters catchment located in Gothic, Colorado, just northeast of Crested Butte (Figure 1). This catchment is representative of many systems supplying the Colorado River, making it an ideal headwater case study. The catchment receives about 0.8 m of precipitation each year, most of which occurs during the winter as snow, with a second peak in precipitation during a late summer monsoon. Heterogeneous geology, variable vegetation, and three life zones—montane, subalpine, and alpine—are modeled at very high resolution (10 m) in order to capture the variability. This allows for examination of the complex controls on hydrologic responses to climate perturbations in headwaters regions.

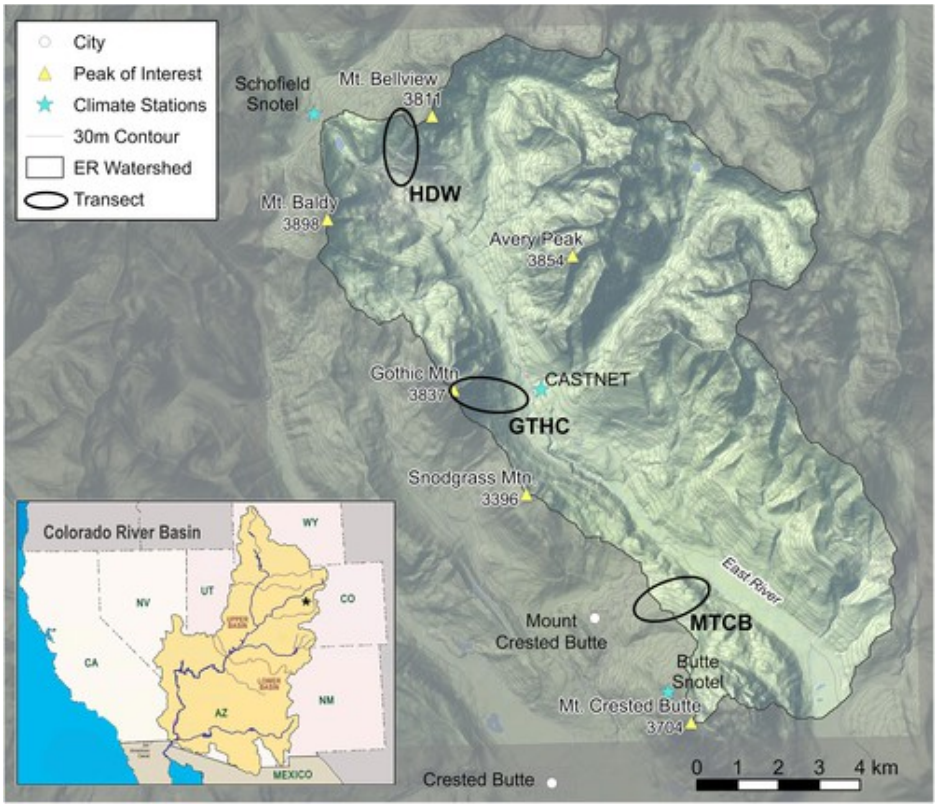

Figure 1

Open in figure viewer
PowerPoint

The study site sits in the headwaters of the Upper Colorado River basin in the south western region of North America. It was chosen as this is emblematic of mountain systems around the world

It is challenging to identify drivers of change from a full catchment response in such heterogeneous regions (Biederman et al., 2014), as well as prohibitively computationally expensive to conduct high resolution

sensitivity analysis on a full watershed. For this reason, we identify three 2D transects that characterize distinct zones within the watershed (Figure 1). The headwaters transect (*HDW*) contributes flow via a steep gradient near the top of the domain, the Gothic Mountain transect (*GTHC*) contributes water to the medium-grade river, and the Mount Crested Butte (*MTCB*) contributes flow to the low-grade meandering floodplain.

Each transect varies in landcover, geology (Table 2), and local climate, allowing for a comparison of these variables under climate perturbations. The headwaters transect (*HDW*) is 1.65 km long and has a 0.48 average slope. This site receives the largest amount of precipitation, about 1.27 m a year, with 68% falling as snow. The Gothic Mountain transect (*GTHC*) is 1.68 km long, has an average slope of 0.63, and receives the least amount of precipitation, about 0.64 m a year, with 38% falling as snow. The Mount Crested Butte (*MTCB*) is 0.98 km long, has an average slope of 0.23, and receives about 0.72 m of precipitation a year, with 64% falling as snow. Land cover was obtained from the National Land Cover Database (NLCD) at 30-m resolution and soil data was obtained from STATSGO2, then bias corrected with land cover and surface geology to include a representation of exposed rock. The surface geology dataset was constructed from US Geological Survey (USGS) geological maps and with corresponding lithologic permeability values obtained from Gleeson et al. (2011). All transects were simulated at 10-m lateral resolution and a variable vertical resolution with thicknesses of 0.1, 0.3, and 0.4 m representing the upper subsurface layers and thickness of 8 and 21 m representing the lower subsurface layers (Table 2).

Table 2. Transect properties including landcover, geology, and soil distributions. Colors indicate location of different geology and soil properties for each transect, consistent with shading of hydraulic conductivity (K [m/h]). The percentage of vegetation within the East River catchment is provided (under ER [%]) to show the prevalence of susceptible grassland within an example Rocky Mountain headwaters system and the representativeness of each transects landcover distribution. Remaining catchment area (<2%) is developed land or existing open shrubland

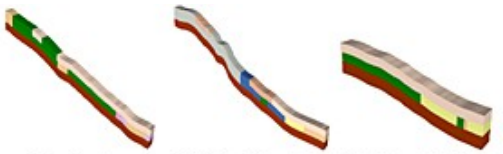

Landcover Type [%]		Headwaters (HDW)	Gothic Mountain (GTHC)	Mt. Crested Butte (MTCB)
	ER [%]			
Grasslands	37	49	20	9
Barren	18	32	41	
Deciduous Broadleaf	15	7	30	52
Evergreen Needleleaf	22		9	34
Wetlands	7			5

Upper Subsurface Layers [%]		HDW	GTHC	MTCB
	K [m/h]			
Sandy Loam	0.02	69	32	100
Mancos Shale	0.02	26		
Undifferentiated	0.2	5		
Crystalline	0.04		38	
Loam	0.15		24	
Talus	0.2		6	

Lower Subsurface Layers [%]		HDW	GTHC	MTCB
	K [m/h]			
Landslide	0.2		11	33
Mancos Shale	0.02	66	4	64
Undifferentiated	0.2	24	13	3
Crystalline	0.04	1	47	
Lower Mancos Shale	0.03	6		
Talus	0.2		25	
Carbonate	0.09	3		

Physical Parameters	HDW	GTHC	MTCB
Length [m]	1650	1680	980
Slope [-]	0.48	0.63	0.23
Average T [°C]	1.1	1.7	3.3
Annual Precipitation [m]	1.27	0.64	0.72

Hourly meteorological forcing is required to drive each of the transect models. Water year 2006 (Oct 2005–Sep 2006) was chosen for this study because precipitation accumulation and temperature were close to the 30-year mean for the region, allowing for an investigation of climate impacts under average conditions. While there is significant year-to-year climate variability in this region, using the same year for both baseline and perturbation scenarios allows for isolation of vegetation and warming impacts, which are difficult to tease out from interannual variability. These observations were obtained using a combination of the US EPA Clean Air Status Trends Network (CASTNET) and two SNOw TELemetry (SNOTEL) sites which are located in the vicinity of the northern and southern most transects (*HDW* and *MTCB*, see Figure 1). The temperature and precipitation data from the CASTNET station were replaced with the corresponding SNOTEL observations.

All transect models have no flow boundary conditions at the base of the subsurface and sides of the domain and an overland flow condition at the base of the slopes. Each transect was spun up (driven to a dynamic equilibrium) where the forcing from WY 2006 (Oct 2005–Sep 2006) were used repeatedly in a continuous simulation until the annual change in storage differed by less than 1% (Kollet & Maxwell, 2008). In addition to this baseline scenario, three perturbations to the WY2006 climate were also simulated: land-cover change where grassland land cover is replaced by shrublands (accomplished by replacing the land-cover types within CLM, based on the findings of (Harte & Shaw, 1995); see Table 1), a warming scenario where a systematic 4 °C

temperature increase is applied, and a scenario that combines these two cases applying both the land cover change and temperature increase. For all perturbed cases, the model was re-spun up using the 1% threshold. While the results presented here are likely different than in a real world scenario where vegetation develops dynamically, simplifying the system to an equilibrium for an anticipated future climate allows for clearer interpretation of related controls on hydrology.

3 RESULTS AND DISCUSSION

The snow and discharge (flow contributing to the stream is calculated as overland flow at the base of each transect) results of all simulation cases are shown in Figure 2. Although there are some commonalities between the responses, the three transects behave quite differently under both natural and perturbation scenarios. Total discharge decreases in all warming cases, and while peak timing shifts earlier for the *HDW* and *MTCB* transects, no change was detected for *GTHC*, which has the least precipitation falling as snow, the steepest slope, and a very different geologic composition (primarily crystalline rock with medium K) from the other transects. This small snowpack and baseflow-driven discharge make *GTHC* less sensitive to snowmelt seasonality in runoff than *HDW* and *MTCB*. The *HDW* (Figure 2a) transect exhibited the largest seasonal variations in streamflow, corresponding to the largest snowpack of all transects. The vegetation scenario resulted in later snowmelt-driven peak flow. This change is in correlation to increased snow water equivalent (SWE) in the summer months, while the overall decrease in discharge is a result of increased total evaporation (Figure 3) both likely tied to greater leaf area index from the shrublands replacing grass. This result is similar to observed reductions in total ET observed when the opposite vegetation shift occurred, from shrubs to grass, in a study across 898 sites by Bradford et al. (2008). The warming and combination scenarios had earlier peak snowmelt and monsoonal discharges due to the earlier snow–rain transition and decreases in snowpack and snow longevity.

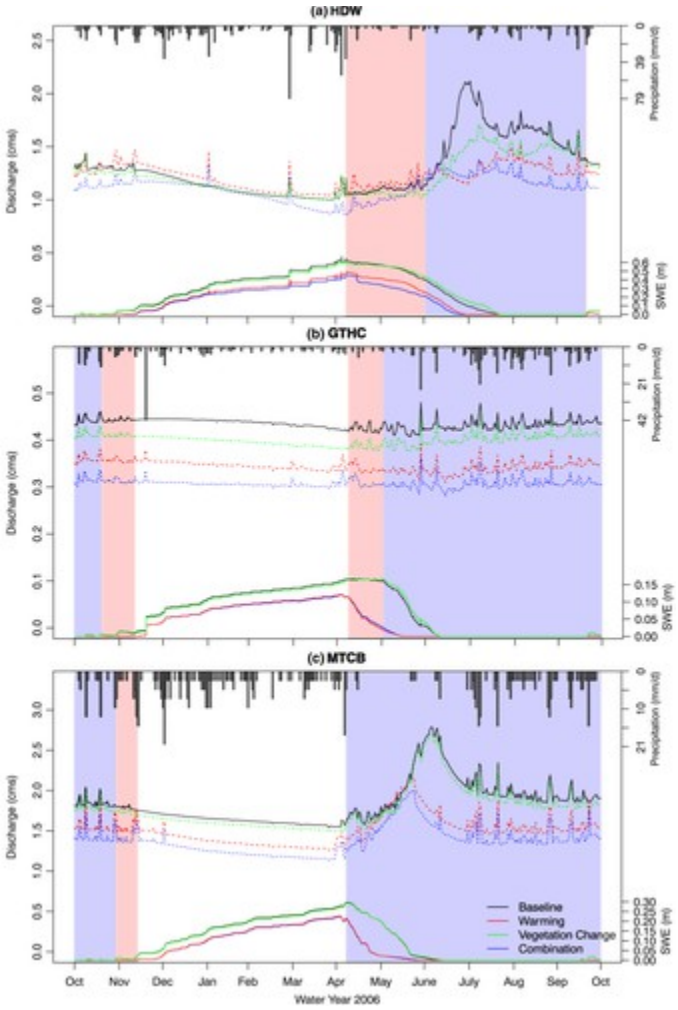

Figure 2

Open in figure viewer
PowerPoint

Plots of daily discharge and SWE demonstrate that while warming has a more pronounced impact on snowpack than vegetation, the response is complex and varies between the Headwaters (a), Gothic (b), and Mount Crested Butte (c) significantly. Note the blue shading that denotes the times when precipitation falls as rain in the baseline case, while the red represents extended rainfall season in the warming case, which also varies between transects due to differences in elevation

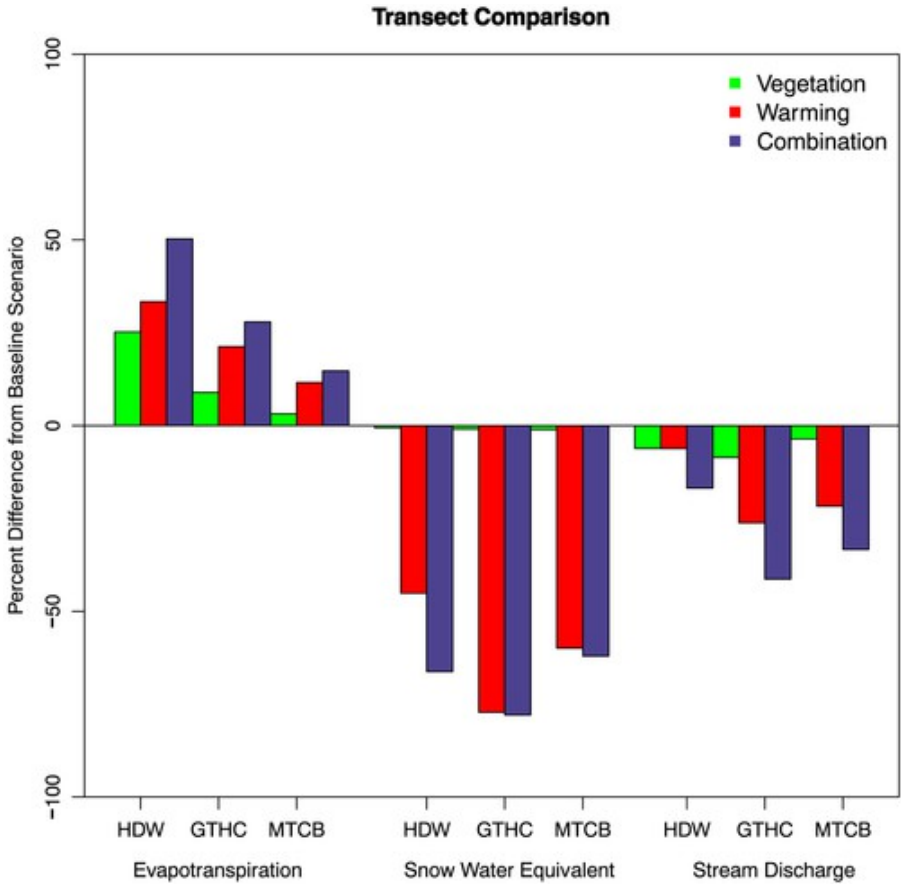

Figure 3

Open in figure viewer
PowerPoint

Annual changes in ET, SWE, and streamflow across all three transects demonstrate that while climate has the largest impact on snow, vegetation changes can have a significant impact on ET and the nonlinearity in response makes predicting system behavior challenging

The *GTHC* transect had small variations in temporal and seasonal changes with discharge, but had large total changes associated with SWE, similar to those of the *HDW* transect (Figure 2b). The vegetation scenario generated a small change in snowpack throughout the winter, while in the early summer it slightly surpassed that of the baseline scenario. The warming and combination scenarios showed large declines in SWE, with snowpack accumulation starting in November, one month later than the baseline, and snowpack depletion occurring in mid May, about one month earlier than the baseline. Timing shifts in discharge at *GTHC* are perhaps muted by the different geology underlying the *GTHC* transect (Table 2c)—a finding consistent with a recent study contrasting response of warming for differing hydrogeology (high conductivity compared to low conductivity) in mountain systems (Markovich et al., 2016)—and the smaller percentage of snowpack and greater fraction of precipitation that falls as rain relative to other transects.

The *MTCB* transect exhibited the smallest discharge response to vegetation change (3.6%) yet had similar changes in timing to that of the HDW transect. This small outflow response is likely caused by the smallest (9%) change in vegetation land cover compared with the other transects (Figure 2c), indicating that in the vegetation case, magnitude of streamflow is sensitive to the extent of vegetation change while timing is much

more sensitive to total snowpack than to slight changes in peak SWE due to canopy shading. The warming and combination scenarios generated large shifts in both SWE and discharge. In the warming scenario, snowpack accumulation began about one month later than baseline but snowmelt occurred at the same time as the baseline scenario; as such, there was no shift in the timing of spring discharge, only the quantity of flow. Timing of discharge peaks for the warming scenario did not change during the monsoonal season, demonstrating event scales dependence on climate more than geology or vegetation. In the fall months, small peaks in stream discharge occurred as a result of the prolonged period where precipitation was falling as rain (see Figure 2c, note the series of isolated discharge peaks).

To help differentiate between stream discharge losses caused by reduced snowpack and higher evapotranspiration (ET), Figure 3 shows percent differences of total ET, SWE, and discharge for each scenario and transect. When comparing the vegetation scenarios between the three transects, results indicate that the percent change in total ET strongly correlates to the amount of vegetation changed on each transect. The largest changes occur in the *HDW* transect (49% vegetation change) and the smallest changes occur on the *MTCB* transect (9% vegetation change). The largest percent change in discharge does not directly correlate to percent change in vegetation, as seen in the *GTHC* transect (20% vegetation change but largest discharge impact). This is due to the climate controls on precipitation partitioning, where in GTHC a small percent change in total ET has a disproportionately large impact on change in discharge since the smaller snowpack at *GTHC* is not a dominant driver of discharge like it is in *HDW* and *MTCB*. This finding that the extent vegetation changes impact hydrologic partitioning is controlled first by changes in climate is corroborated by other observational and modeling studies (Bradford et al., 2008, Troch, Carrillo, Sivapalan, Wagener, & Sawicz, 2013).

The *HDW* transect had the largest evaporative increases for the warming scenario with the changes in the *MTCB* transect being the smallest. However, the largest decreases in SWE and discharge were seen in the *GTHC* and *MTCB* transects, with the *GTHC* transect, which has the least SWE for the baseline case, having a slightly larger decrease in discharge. The combination scenario had larger percent changes, and a bigger impact on SWE and discharge, than the vegetation or warming scenarios independently. Most importantly, the impact of the combination is greater than the sum of the impact from each change independently, implying a nonlinear feedback between warming temperature and vegetation shifts. Field observations of snowpack under beetle-killed trees suggest that changes in ground exposure, and thus sublimation, offsets changes in interception and ultimately minimize differences in SWE with canopy loss (Biederman et al., 2014). When combined with a warming climate, however, the decrease in available energy with increased LAI may amplify the effects of canopy loss, with the effects becoming particularly apparent after exceeding the amount offset by the change in interception. In such a complex system, it is uncertain how this feedback between vegetation and climate would change if it were possible to accurately represent vegetation succession dynamically in the model. It is possible that warming driven changes in vegetation would occur faster due to the positive feedback between warming and shifts from grasslands to shrubs on moisture availability.

Figure 4 plots the daily, spatially averaged soil saturation in the top model cells for each scenario by transect. Here, the *HDW* transect behaves differently than *GTHC* and *MTCB*, with more pronounced changes during the winter months under temperature increases and greater variability in response from all cases during summer

months. Both the *GTHC* and *MTCB* transects experienced only minor changes in soil saturation due to vegetation changes and see a lengthening of a dry period between the snowmelt signal and monsoon. In the vegetation scenarios, regardless of the amount of vegetation change, interception, transpiration, and total evaporation increased for each transect; however, soil moisture only decreased in the transects with the greatest vegetation change (*HDW* and *GTHC*), indicating that changes in soil moisture are slightly less sensitive than expected from changes in ET to vegetation shifts. These soil moisture decreases correspond to the largest increases in total evaporation seen in Figure 3, a result of spring and summer plant productivity due to increased energy. After the monsoonal rains began, soil saturation returned to baseline conditions. These changes were a result of increased water demand and interception from the open shrublands as they have a larger canopy than the grasslands. Increased canopy allows for an increase in interception of precipitation and an increase in transpiration. Increased canopy cover also provides vegetative shading and greater snowpack found in between and below the shrubs, though this small persistence of snowpack was not enough to compensate for water loss in the summer due to increased ET. In the winter, the increased canopy causes a lag in snowpack development due to increased interception and the lower snowpack (Figure 2). While these changes were present in each transect, the magnitude did not respond equally throughout the catchment. The effect from vegetation depended on the differences in extent of vegetation change and climate more than geology for each transect. The largest vegetation and ET changes were seen in the *HDW* transect; however, the largest relative discharge change was seen in the *GTHC* transect. *GTHC* had an 8.6% decrease in discharge, which is 2% larger than *HDW* and 5% larger than *MTCB*. This outcome is likely because *GTHC* receives the least precipitation (Table 2d) and the least amount of precipitation that falls as snow, making streamflow more sensitive to a smaller change in vegetation. These forcing, flow, and saturation differences make *GTHC* a moisture-limited system and therefore generate an increased response in discharge. The saturation for the *MTCB* transect was the least impacted which is likely a result of the minimal vegetative change.

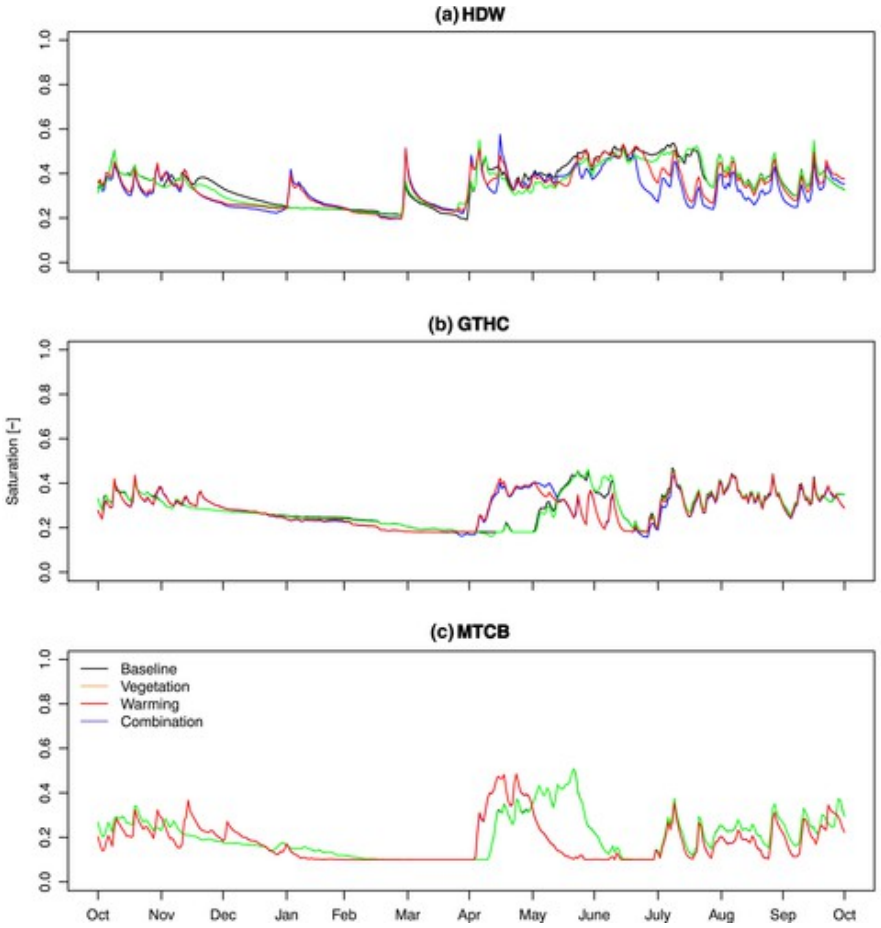

Figure 4

Open in figure viewer
PowerPoint

The impacts of vegetation and climate are more mixed for the headwaters transect (a), but there is a clear decrease in plant-available moisture between the snowmelt and monsoon signal under the climate scenario for the Gothic and Mount Crested Butte transects (b-c). This underscores the natural variability in response across portions of the catchment

The warming scenario caused an increase in ET and an earlier snow transition to rainfall. These changes stemmed from an increase in the atmospheric moisture deficit as well as depleted snowpack, a result of the delayed snowfall, increased sublimation, and increased snow-rain transition. All of these changes amounted to a larger system response in discharge and storage depletions than the vegetation scenario across all transects. In the *HDW* transect, spikes in soil moisture can be found in the winter as some days exceeded critical temperatures initiating snowmelt, also seen as the isolated winter hydrograph peaks in Figure 2a. In the summer months, saturation had an overall decline, but spiked during precipitation events.

Generally, these results indicate warming plays a larger role than vegetation change, but the combination of the two amplifies the hydrologic response. This is consistent with previous studies demonstrating that the impacts of vegetation changes on hydrologic partitioning depend strongly on climate changes (Bradford et al., 2008, Troch et al., 2013). In addition, model results suggest that each hillslope transect responds differently depending on its orographic location, land cover, soil, and geologic properties. The discharge patterns for each transect can be tracked in their respective soil moisture patterns. Soil moisture is also an indicator of how

much water is available for vegetative and atmospheric uptake. It is also evident, as discussed above, that vegetation change further enhances the changes generated from the warming scenario alone, which could exacerbate the speed of vegetation transition as natural vegetation change is unlikely to occur without increased warming.

The hydrologic responses perturbed from temperature increases shown here (e.g. snow depletions, earlier melt time, precipitation transitions, and decreased discharge) are similar to prior studies. These results also correspond with those seen in the meadow warming experiments, such as the tie between decreased soil moisture and increased ET (Harte & Shaw, 1995). The use of field study results such as those from the meadow warming experiments further enhanced model predictions of a future climate as the inclusion of vegetation change with warming predictions caused additional decreases in discharge by 10–15%.

4 CONCLUSIONS

In this study, a high-resolution, integrated hydrologic model was used to study the impact of hydrologic response under increased warming, vegetation change and the combination of the two. These climate induced changes resulted in earlier peak streamflow timing in two transects and decreases in discharge and storage across all three transects. The addition of vegetation change to increased warming projections led to additional losses in streamflow likely due to intensified evaporative losses. Overall, discharge and storage losses equated to 4–41% and 1–4%, respectively. Vegetation changes had a measurable, but small impact on SWE, while warming had a more significant impact, with up to a 75% decrease in snowpack. This is consistent with modeling studies of insect-induced land cover change (Mikkelson et al., 2013, Penn et al., 2016) where there is a combination of increased canopy interception reducing snowpack accumulation in winter months and increased shading allowing that snowpack to persist longer. ET increased for all scenarios and these changes were dominated by temperature with nonlinear increases resulting from the combined perturbation.

Prior studies (Edburg et al., 2012, Williams et al., 2013) have linked tree mortality to both increased temperature and extended periods of decreased soil moisture and similar changes are seen in the simulation results presented here. While these integrated model simulations represent many complex processes and their interactions—including land cover, surface and subsurface heterogeneity—they are inherently simplifications of a complex natural system. Dynamic linkages between vegetation productivity and succession and climate change not modeled explicitly here might further complicate this story. Likewise, the substantial variability seen between the three transects simulated here is not intended as a comprehensive representation of the full spectrum present among mountain headwater systems even across western North America.

We see three distinct conclusions from this work: (a) warming generally outpaces vegetation changes and causes a larger impact to hydrology in mountain systems; (b) the combined effects of vegetation change and warming amplify to create a larger, nonlinear response than either component individually; and (c) variability among transects and thus within a single headwaters system creates a range of responses to perturbation that is a function of not only precipitation and microclimate but slope, geology, and land cover. These trends can

help inform water and forest management practices as well as future studies of climate change in critical headwaters regions.

ACKNOWLEDGMENTS

This work is based upon work supported as part of the Sustainable Systems Scientific Focus Area funded by the U.S. Department of Energy, Office of Science, Office of Biological and Environmental Research under Award Number DE-AC02-05CH11231. The authors declare no conflicts of interest or competing financial interest. We thank the anonymous reviewers for their constructive comments, which have improved the quality and clarity of this work.

REFERENCES

1. Adams, H. D., Luce, C. H., Breshears, D. D., Allen, C. D., Weiler, M., Hale, V. C., … Huxman, T. E. (2012). Ecohydrological consequences of drought- and infestation-triggered tree die-off: Insights and hypotheses. *Ecohydrology*, **5**(2), 145–159.

2. Allen, C. D., Macalady, A. K., Chenchouni, H., Bachelet, D., McDowell, N., Vennetier, M., … Cobb, N. (2010). A global overview of drought and heat-induced tree mortality reveals emerging climate change risks for forests. *Forest Ecology and Management*, **259**(4), 660–684.

3. Bales, R. C., Molotch, N. P., Painter, T. H., Dettinger, M. D., Rice, R., & Dozier, J. (2006). Mountain hydrology of the western United States. *Water Resources Research*, **42**(8).

4. Bearup, L. A., Maxwell, R. M., Clow, D. W., & McCray, J. E. (2014). Hydrological effects of forest transpiration loss in bark beetle-impacted watersheds. *Nature Climate Change*, **4**(6), 481–486.

5. Berghuijs, W. R., Woods, R. A., & Hrachowitz, M. (2014). A precipitation shift from snow towards rain leads to a decrease in streamflow. *Nature Climate Change*, **4**(7), 583–586.

6. Biederman, J. A., Harpold, A. A., Gochis, D. J., Ewers, B. E., Reed, D. E., Papuga, S. A., & Brooks, P. D. (2014). Increased evaporation following widespread tree mortality limits streamflow response. *Water Resources Research*, **50**(7), 5395–5409.

7. Bradford, J. B., Birdsey, R. A., Joyce, L. A., & Ryan, M. G. (2008). Tree age, disturbance history, and carbon stocks and fluxes in subalpine Rocky Mountain forests. *Global Change Biology*, **14**(12), 2882–2897.

8. Clow, D. W. (2009). Changes in the timing of snowmelt and streamflow in Colorado: A response to recent warming. *Journal of Climate*, **23**(9), 2293–2306.

9. Edburg, S. L., Hicke, J. A., Brooks, P. D., Pendall, E. G., Ewers, B. E., Norton, U., … Meddens, A. J. H. (2012). Cascading impacts of bark beetle-caused tree mortality on coupled biogeophysical and biogeochemical processes. *Frontiers in Ecology and the Environment*, **10**(8), 416–424.

10. Foster, L. M., Bearup, L. A., Molotch, N. P., Brooks, P. D., & Maxwell, R. M. (2016). Energy budget increases reduce mean streamflow more than snow-rain transitions: Using integrated modeling to isolate climate change impacts on Rocky Mountain hydrology. *Environmental Research Letters*, **11**(40). doi:10.1088/1748-9326/11/4/044015

11. Gleeson, T., Smith, L., Moosdorf, N., Hartmann, J., Dürr, H. H., Manning, A. H., … Jellinek, A. M. (2011). Mapping permeability over the surface of the Earth. *Geophysical Research Letters*, **38**(2), L02401.

12. Goulden, M. L., & Bales, R. C. (2014). Mountain runoff vulnerability to increased evapotranspiration with vegetation expansion. *Proceedings of the National Academy of Sciences*, **111**(39), 14071–14075.

13. Hansen, M. C., Potapov, P. V., Moore, R., Hancher, M., Turubanova, S. A., Tyukavina, A., … Townshend, J. R. G. (2013). High-resolution global maps of 21st-century forest cover change. *Science*, **342**(6160), 850–853.

14. Harte, J., & Shaw, R. (1995). Shifting dominance within a montane vegetation community: Results of a climate-warming experiment. *Science*, **267**(5199), 876–880.

15. Jefferson, J. L., & Maxwell, R. M. (2015). Evaluation of simple to complex parameterizations of bare ground evaporation. *Journal of Advances in Modeling Earth Systems*, **7**(3), 1075–1092.

16. Jefferson, J. L., Gilbert, J. M., Constantine, P. G., & Maxwell, R. M. (2015). Active subspaces for sensitivity analysis and dimension reduction of an integrated hydrologic model. *Computers & Geosciences*, **83**, 127–138.

17. Kollet, S. J., & Maxwell, R. M. (2006). Integrated surface-groundwater flow modeling: A free-surface overland flow boundary condition in a parallel groundwater flow model. *Advances in Water Resources*, **29**(7), 945–958.

18. Kollet, S. J., & Maxwell, R. M. (2008). Capturing the influence of groundwater dynamics on land surface processes using an integrated, distributed watershed model. *Water Resources Research*, **44**(W02402), 18.

19. Lukas, J., J. Barsugli, I. Rangwala & K. Woler (2014). Climate change in Colorado: A synthesis to support water resources management and adaptation, western water assessment, Cooperative Institute for Research in Environmental Sciences (CIRES), University of Colorado Boulder: 108.

20. Markovich, K. H., Maxwell, R. M., & Fogg, G. E. (2016). Hydrogeological response to climate change in alpine hillslopes. *Hydrological Processes*, **30**, 3126–3138.

21. Mikkelson, K. M., Maxwell, R. M., Ferguson, I., Stednick, J. D., McCray, J. E., & Sharp, J. O. (2013). Mountain pine beetle infestation impacts: Modeling water and energy budgets at the hill-slope scale. *Ecohydrology*, **6**(1), 64–72.

22. Penn, C. A., Bearup, L. A., Maxwell, R. M., & Clow, D. W. (2016). Numerical experiments to explain multiscale hydrological responses to mountain pine beetle tree mortality in a headwater watershed. *Water Resources Research*, **52**(4), 3143–3161.

23. Troch, P. A., Carrillo, G., Sivapalan, M., Wagener, T., & Sawicz, K. (2013). Climate–vegetation–soil interactions and long-term hydrologic partitioning: Signatures of catchment co-evolution. *Hydrology and Earth System Sciences*, **17**(6), 2209–2217.

24. Vano, J. A., Udall, B., Cayan, D. R., Overpeck, J. T., Brekke, L. D., Das, T., … Lettenmaier, D. P. (2013). Understanding uncertainties in Future Colorado River Streamflow. *Bulletin of the American Meteorological Society*, **95**(1), 59–78.

25. Williams, P. A., Allen, C. D., Macalady, A. K., Griffin, D., Woodhouse, C. A., Meko, D. M., … McDowell, N. G. (2013). Temperature as a potent driver of regional forest drought stress and tree mortality. *Nature Climate Change*, **3**(3), 292–297.